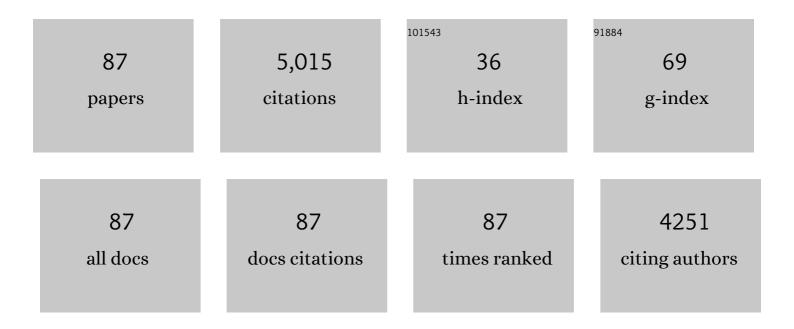
## Richard Kijowski

List of Publications by Year in descending order

Source: https://exaly.com/author-pdf/3673683/publications.pdf Version: 2024-02-01



#	Article	IF	CITATIONS
1	Deep Learning MR Imaging–based Attenuation Correction for PET/MR Imaging. Radiology, 2018, 286, 676-684.	7.3	315
2	Deep convolutional neural network and 3D deformable approach for tissue segmentation in musculoskeletal magnetic resonance imaging. Magnetic Resonance in Medicine, 2018, 79, 2379-2391.	3.0	240
3	Effects of refocusing flip angle modulation and view ordering in 3D fast spin echo. Magnetic Resonance in Medicine, 2008, 60, 640-649.	3.0	239
4	Knee Joint: Comprehensive Assessment with 3D Isotropic Resolution Fast Spin-Echo MR Imaging—Diagnostic Performance Compared with That of Conventional MR Imaging at 3.0 T. Radiology, 2009, 252, 486-495.	7.3	238
5	Deep Learning Approach for Evaluating Knee MR Images: Achieving High Diagnostic Performance for Cartilage Lesion Detection. Radiology, 2018, 289, 160-169.	7.3	193
6	Juvenile versus Adult Osteochondritis Dissecans of the Knee: Appropriate MR Imaging Criteria for Instability. Radiology, 2008, 248, 571-578.	7.3	191
7	Evaluation of the Articular Cartilage of the Knee Joint: Value of Adding a T2 Mapping Sequence to a Routine MR Imaging Protocol. Radiology, 2013, 267, 503-513.	7.3	158
8	Comparison of 1.5- and 3.0-T MR Imaging for Evaluating the Articular Cartilage of the Knee Joint. Radiology, 2009, 250, 839-848.	7.3	152
9	Deep convolutional neural network for segmentation of knee joint anatomy. Magnetic Resonance in Medicine, 2018, 80, 2759-2770.	3.0	148
10	Magnetic resonance imaging of the elbow. Part II: Abnormalities of the ligaments, tendons, and nerves. Skeletal Radiology, 2005, 34, 1-18.	2.0	146
11	MR Diagnosis of Posterior Root Tears of the Lateral Meniscus Using Arthroscopy as the Reference Standard. American Journal of Roentgenology, 2009, 192, 480-486.	2.2	142
12	MRI Findings of Osteochondritis Dissecans of the Capitellum with Surgical Correlation. American Journal of Roentgenology, 2005, 185, 1453-1459.	2.2	137
13	Arthroscopic Validation of Radiographic Grading Scales of Osteoarthritis of the Tibiofemoral Joint. American Journal of Roentgenology, 2006, 187, 794-799.	2.2	128
14	Subchondral Bone Marrow Edema in Patients with Degeneration of the Articular Cartilage of the Knee Joint. Radiology, 2006, 238, 943-949.	7.3	115
15	Validation of MRI Classification System for Tibial Stress Injuries. American Journal of Roentgenology, 2012, 198, 878-884.	2.2	96
16	State of the Art: Imaging of Osteoarthritis—Revisited 2020. Radiology, 2020, 296, 5-21.	7.3	96
17	Fully Automated Diagnosis of Anterior Cruciate Ligament Tears on Knee MR Images by Using Deep Learning. Radiology: Artificial Intelligence, 2019, 1, 180091.	5.8	94
18	Magnetic resonance imaging findings in patients with medial epicondylitis. Skeletal Radiology, 2005, 34, 196-202.	2.0	89

#	Article	IF	CITATIONS
19	Routine 3D magnetic resonance imaging of joints. Journal of Magnetic Resonance Imaging, 2011, 33, 758-771.	3.4	89
20	Vastly Undersampled Isotropic Projection Steady-State Free Precession Imaging of the Knee: Diagnostic Performance Compared with Conventional MR. Radiology, 2009, 251, 185-194.	7.3	88
21	A deep learning approach for 18F-FDG PET attenuation correction. EJNMMI Physics, 2018, 5, 24.	2.7	88
22	Radiographic Findings of Osteoarthritis versus Arthroscopic Findings of Articular Cartilage Degeneration in the Tibiofemoral Joint. Radiology, 2006, 239, 818-824.	7.3	87
23	Radiography of the elbow for evaluation of patients with osteochondritis dissecans of the capitellum. Skeletal Radiology, 2005, 34, 266-271.	2.0	78
24	MANTIS: Modelâ€Augmented Neural neTwork with Incoherent <i>k</i> â€space Sampling for efficient MR parameter mapping. Magnetic Resonance in Medicine, 2019, 82, 174-188.	3.0	77
25	Magnetic resonance imaging of the elbow. Part I: Normal anatomy, imaging technique, and osseous abnormalities. Skeletal Radiology, 2004, 33, 685-697.	2.0	71
26	SANTIS: Samplingâ€Augmented Neural neTwork with Incoherent Structure for MR image reconstruction. Magnetic Resonance in Medicine, 2019, 82, 1890-1904.	3.0	70
27	Knee imaging: Rapid threeâ€dimensional fast spinâ€echo using compressed sensing. Journal of Magnetic Resonance Imaging, 2017, 45, 1712-1722.	3.4	63
28	Evaluation of the menisci of the knee joint using three-dimensional isotropic resolution fast spin-echo imaging: diagnostic performance in 250 patients with surgical correlation. Skeletal Radiology, 2012, 41, 169-178.	2.0	61
29	3.0-T Evaluation of Knee Cartilage by Using Three-Dimensional IDEAL GRASS Imaging: Comparison with Fast Spin-Echo Imaging. Radiology, 2010, 255, 117-127.	7.3	55
30	Deep Learning for Lesion Detection, Progression, and Prediction of Musculoskeletal Disease. Journal of Magnetic Resonance Imaging, 2020, 52, 1607-1619.	3.4	55
31	Magnetic resonance imaging findings in patients with peroneal tendinopathy and peroneal tenosynovitis. Skeletal Radiology, 2007, 36, 105-114.	2.0	50
32	Clinical Usefulness of Adding 3D Cartilage Imaging Sequences to a Routine Knee MR Protocol. American Journal of Roentgenology, 2011, 196, 159-167.	2.2	45
33	Bicomponent ultrashort echo time analysis for assessment of patients with patellar tendinopathy. Journal of Magnetic Resonance Imaging, 2017, 46, 1441-1447.	3.4	45
34	Arthroscopic Partial Meniscectomy: MR Imaging for Prediction of Outcome in Middle-Aged and Elderly Patients. Radiology, 2011, 259, 203-212.	7.3	44
35	Magnetic resonance parameter mapping using modelâ€guided selfâ€supervised deep learning. Magnetic Resonance in Medicine, 2021, 85, 3211-3226.	3.0	41
36	Correlation between radiographic findings of osteoarthritis and arthroscopic findings of articular cartilage degeneration within the patellofemoral joint. Skeletal Radiology, 2006, 35, 895-902.	2.0	40

#	Article	IF	CITATIONS
37	Analysis of mcDESPOT―and CPMGâ€derived parameter estimates for twoâ€component nonexchanging systems. Magnetic Resonance in Medicine, 2016, 75, 2406-2420.	3.0	40
38	Clinical Cartilage Imaging of the Knee and Hip Joints. American Journal of Roentgenology, 2010, 195, 618-628.	2.2	36
39	Rapid multicomponent T2 analysis of the articular cartilage of the human knee joint at 3.0T. Journal of Magnetic Resonance Imaging, 2014, 39, 1191-1197.	3.4	36
40	Evaluation of the articular cartilage of the knee joint with vastly undersampled isotropic projection reconstruction steady-state free precession imaging. Journal of Magnetic Resonance Imaging, 2006, 24, 168-175.	3.4	35
41	Cartilage morphology at 3.0T: Assessment of threeâ€dimensional magnetic resonance imaging techniques. Journal of Magnetic Resonance Imaging, 2010, 32, 173-183.	3.4	35
42	Diagnostic Performance of Three-dimensional MRI for Depicting Cartilage Defects in the Knee: A Meta-Analysis. Radiology, 2018, 289, 71-82.	7.3	35
43	The Role of Ultrasound in the Evaluation of Sports Medicine Injuries of the Upper Extremity. Clinics in Sports Medicine, 2006, 25, 569-590.	1.8	34
44	Significance of radiographic abnormalities in patients with tibial stress injuries: correlation with magnetic resonance imaging. Skeletal Radiology, 2007, 36, 633-640.	2.0	34
45	Short-term Clinical Importance of Osseous Injuries Diagnosed at MR Imaging in Patients with Anterior Cruciate Ligament Tear. Radiology, 2012, 264, 531-541.	7.3	33
46	Pediatric Throwing Injuries of the Elbow. Seminars in Musculoskeletal Radiology, 2010, 14, 419-429.	0.7	32
47	Improved fat suppression using multipeak reconstruction for IDEAL chemical shift fatâ€water separation: Application with fast spin echo imaging. Journal of Magnetic Resonance Imaging, 2009, 29, 436-442.	3.4	28
48	Evaluation of trabecular microarchitecture in nonosteoporotic postmenopausal women with and without fracture. Journal of Bone and Mineral Research, 2012, 27, 1494-1500.	2.8	28
49	Articular Cartilage of the Human Knee Joint: In Vivo Multicomponent T2 Analysis at 3.0 T. Radiology, 2015, 277, 477-488.	7.3	28
50	Rapid multicomponent relaxometry in steady state with correction of magnetization transfer effects. Magnetic Resonance in Medicine, 2016, 75, 1423-1433.	3.0	25
51	Diagnosis of Knee Meniscal Injuries by Using Three-dimensional MRI: A Systematic Review and Meta-Analysis of Diagnostic Performance. Radiology, 2019, 290, 435-445.	7.3	25
52	Cruciate ligament injuries of the knee: A metaâ€analysis of the diagnostic performance of 3D MRI. Journal of Magnetic Resonance Imaging, 2019, 50, 1545-1560.	3.4	24
53	Cartilage imaging at 3.0T with gradient refocused acquisition in the steadyâ€state (GRASS) and IDEAL fatâ€water separation. Journal of Magnetic Resonance Imaging, 2008, 28, 167-174.	3.4	23
54	Optimizing isotropic three-dimensional fast spin-echo methods for imaging the knee. Journal of Magnetic Resonance Imaging, 2014, 39, 1417-1425.	3.4	22

#	Article	IF	CITATIONS
55	Artificial intelligence in musculoskeletal imaging: a perspective on value propositions, clinical use, and obstacles. Skeletal Radiology, 2022, 51, 239-243.	2.0	22
56	Effect of Loading on In Vivo Tibiofemoral and Patellofemoral Kinematics of Healthy and ACL-Reconstructed Knees. American Journal of Sports Medicine, 2017, 45, 3272-3279.	4.2	21
57	MRI Characteristics of Healed and Unhealed Peripheral Vertical Meniscal Tears. American Journal of Roentgenology, 2014, 202, 585-592.	2.2	20
58	Evaluation of the Articular Cartilage of the Knee Joint Using an Isotropic Resolution 3D Fast Spin-Echo Sequence With Conventional and Radial Reformatted Images. American Journal of Roentgenology, 2015, 205, 371-379.	2.2	20
59	The Clinical Significance of Dark Cartilage Lesions Identified on MRI. American Journal of Roentgenology, 2015, 205, 1251-1259.	2.2	19
60	American Society of Biomechanics Clinical Biomechanics Award 2015: MRI assessments of cartilage mechanics, morphology and composition following reconstruction of the anterior cruciate ligament. Clinical Biomechanics, 2016, 34, 38-44.	1.2	19
61	Juvenile Osteochondritis Dissecans: Cartilage T2 Mapping of Stable Medial Femoral Condyle Lesions. Radiology, 2018, 288, 536-543.	7.3	19
62	Osteochondritis Dissecans of the Elbow in Children: MRI Findings of Instability. American Journal of Roentgenology, 2019, 213, 1145-1151.	2.2	19
63	High-performance rapid MR parameter mapping using model-based deep adversarial learning. Magnetic Resonance Imaging, 2020, 74, 152-160.	1.8	19
64	Morphologic Imaging of Articular Cartilage. Magnetic Resonance Imaging Clinics of North America, 2011, 19, 229-248.	1.1	17
65	MRI characteristics of torn and untorn post-operative menisci. Skeletal Radiology, 2017, 46, 1353-1360.	2.0	17
66	The Clinical Significance of Osteophytes in Compartments of the Knee Joint With Normal Articular Cartilage. American Journal of Roentgenology, 2018, 210, W164-W171.	2.2	17
67	Assessment of different fitting methods for in-vivo bi-component T2* analysis of human patellar tendon in magnetic resonance imaging. Muscles, Ligaments and Tendons Journal, 2017, 7, 163.	0.3	16
68	American Society of Biomechanics Clinical Biomechanics Award 2017: Non-anatomic graft geometry is linked with asymmetric tibiofemoral kinematics and cartilage contact following anterior cruciate ligament reconstruction. Clinical Biomechanics, 2018, 56, 75-83.	1.2	16
69	Accuracy of model-based tracking of knee kinematics and cartilage contact measured by dynamic volumetric MRI. Medical Engineering and Physics, 2016, 38, 1131-1135.	1.7	15
70	Preoperative MRI Shoulder Findings Associated with Clinical Outcome 1 Year after Rotator Cuff Repair. Radiology, 2019, 291, 722-729.	7.3	14
71	Anterior Cruciate Ligament Graft Tunnel Placement and Graft Angle Are Primary Determinants of Internal Knee Mechanics After Reconstructive Surgery. American Journal of Sports Medicine, 2020, 48, 3503-3514.	4.2	14
72	Quantitative Magnetic Resonance Imaging of the Articular Cartilage of the Knee Joint. Magnetic Resonance Imaging Clinics of North America, 2014, 22, 649-669.	1.1	12

#	Article	IF	CITATIONS
73	Risks and Benefits of Intra-articular Corticosteroid Injection for Treatment of Osteoarthritis: What Radiologists and Patients Need to Know. Radiology, 2019, 293, 664-665.	7.3	11
74	3D MRI of Articular Cartilage. Seminars in Musculoskeletal Radiology, 2021, 25, 397-408.	0.7	11
75	Rapid isotropic resolution cartilage assessment using radial alternating repetition time balanced steadyâ€state freeâ€precession imaging. Journal of Magnetic Resonance Imaging, 2014, 40, 796-803.	3.4	9
76	Maturation-Related Changes in T2 Relaxation Times of Cartilage and Meniscus of the Pediatric Knee Joint at 3 T. American Journal of Roentgenology, 2018, 211, 1369-1375.	2.2	9
77	Multicomponent <i>T</i> <sub>2</sub> analysis of articular cartilage with synovial fluid partial volume correction. Journal of Magnetic Resonance Imaging, 2016, 43, 1140-1147.	3.4	7
78	Rapid single scan ramped hybridâ€encoding for bicomponent T2* mapping in a human knee joint: A feasibility study. NMR in Biomedicine, 2020, 33, e4391.	2.8	7
79	Dual halfâ€echo phase correction for implementation of 3D radial SSFP at 3.0 T. Magnetic Resonance in Medicine, 2010, 63, 282-289.	3.0	6
80	Rapid in vivo multicomponent <i>T</i> <sub>2</sub> mapping of human knee menisci. Journal of Magnetic Resonance Imaging, 2015, 42, 1321-1328.	3.4	6
81	Volumetric Magnetic Resonance Imaging of the Musculoskeletal System. Seminars in Roentgenology, 2013, 48, 140-147.	0.6	4
82	Utilization of a balanced steady state free precession signal model for improved fat/water decomposition. Magnetic Resonance in Medicine, 2016, 75, 1269-1277.	3.0	4
83	Three-Dimensional Magnetic Resonance Imaging of Joints. Topics in Magnetic Resonance Imaging, 2010, 21, 297-313.	1.2	3
84	Bi-component T2 mapping correlates with articular cartilage material properties. Journal of Biomechanics, 2021, 116, 110215.	2.1	2
85	Standardization of Compositional MRI of Knee Cartilage: Why and How. Radiology, 2021, 301, 433-434.	7.3	2
86	Proximal forearm extensor muscle strain is reduced when driving nails using a shock-controlled hammer. Clinical Biomechanics, 2016, 38, 22-28.	1.2	1
87	Imaging of Track and Field Injuries. , 2016, , 623-640.		О